

## Hydrogen-Bond Acceptor Properties of Nitro-O Atoms: A Combined Crystallographic Database and *Ab Initio* Molecular Orbital Study

FRANK H. ALLEN,<sup>a\*</sup> CHRISTINE A. BAALHAM,<sup>a</sup> JOS P. M. LOMMERSE,<sup>a</sup> PAUL R. RAITHBY<sup>b</sup> AND EMMA SPARR<sup>b†</sup>

<sup>a</sup>Cambridge Crystallographic Data Centre, 12 Union Road, Cambridge CB2 1EZ, England, and <sup>b</sup>Department of Chemistry, University of Cambridge, Lensfield Road, Cambridge CB2 1EW, England.

E-mail: allen@ccdc.cam.ac.uk

(Received 2 June 1997; accepted 15 July 1997)

### Abstract

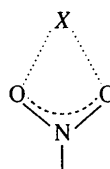
Crystallographic data for 620 C—nitro-O···H—N,O hydrogen bonds, involving 560 unique H atoms, have been investigated to the van der Waals limit of 2.62 Å. The overall mean nitro-O···H bond length is 2.30 (1) Å, which is much longer (weaker) than comparable hydrogen bonds involving >C=O acceptors in ketones, carboxylic acids and amides. The donor hydrogen prefers to approach the nitro-O atoms in the C—NO<sub>2</sub> plane and there is an approximate 3:2 preference for hydrogen approach between the two nitro-O atoms, rather than between the C and O substituents. However, hydrogen approach between the two O acceptors is usually strongly asymmetric, the H atom being more closely associated with one of the O atoms: only 60 H atoms have both O···H distances ≤ 2.62 Å. The approach of hydrogen along putative O-atom lone-pair directions is clearly observed. *Ab-initio*-based molecular orbital calculations (6-31G\*\* basis set level), using intermolecular perturbation theory (IMPT) applied to the nitromethane–methanol model dimer, agree with the experimental observations. IMPT calculations yield an attractive hydrogen-bond energy of *ca* −15 kJ mol<sup>−1</sup>, about half as strong as the >C=O···H bonds noted above.

### 1. Introduction

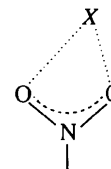
In recent years, non-covalent interactions between carbon-bound I atoms and the O atoms of nitro groups have been used to engineer crystals that contain predictable packing motifs in their extended structures. Thus, the 1:1 complex of 1,4-diiodobenzene and 1,4-dinitrobenzene (Allen, Goud, Hoy, Howard & Desiraju, 1994), 4-iodonitrobenzene, and the 1:2 complex of 1,4-dinitrobenzene and 4-iodocinnamic acid (Thalladi *et al.*, 1996) each contain symmetric or near-symmetric examples of the bifurcated I···O(nitro) motif (I). The fact that motif (I) maintains its integrity, even in the presence of

the more energetically favourable carboxylic acid dimer motif in the cinnamic acid structure, has led Desiraju (1995) to include motif (I) in a list of supramolecular synthons that are important in crystal engineering and other molecular recognition processes.

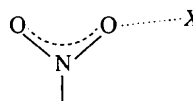
As part of these studies, Allen, Lommerse, Hoy, Howard & Desiraju (1997) recently carried out a combined crystallographic database and *ab-initio*-based molecular orbital study of the generalized C—X···O(nitro)—C synthon (X = Cl, Br, I). This work indicated that two principal interaction motifs exist in crystal structures, the bifurcated motif in its symmetric (I) and asymmetric (II) forms, and the mono-coordinate motif (III). Motif (III) was preferred for the smaller Cl



(I), X = H, Cl, Br, I



(II), X = H, Cl, Br, I



(III), X = H, Cl, Br, I

atom, but Br and, particularly, I showed a preference for motif (I). The larger size of I makes it easier for this atom to form symmetric or near-symmetric interactions with both nitro-O atoms. Further, the computational work showed that the attractive Cl···O(nitro) interaction energy was *ca* −6 kJ mol<sup>−1</sup> [motif (III), 6-31G\* basis set level], with larger values implied for the larger halogens on the basis of the limited calculations that were possible for Br at the [6s4p1d] basis set level. The Cl···O(nitro) interaction energy was considerably lower than the −10 kJ mol<sup>−1</sup> computed at the 6-31G\* basis set level, and using the same software, for a C—Cl···O=C interaction by Lommerse, Stone, Taylor & Allen (1996).

† Undergraduate Visitor from University of Lund. Present Address: Physical Chemistry 1, Chemical Center, PO Box 124, University of Lund, S-22100 Lund, Sweden.

As the  $\text{Cl}\cdots\text{O}$  interactions were shown to be predominantly electrostatic in nature, the latter result implied that hydrogen bonds to nitro-O atoms from strong donors, e.g.  $\text{O—H}$  or  $\text{N—H}$ , would be weaker than those to O atoms from carbonyl groups in e.g. ketones, carboxylic acids or amides. However, reference to Jeffrey & Saenger (1991) shows that hydrogen-bond formation to nitro-O acceptors has received relatively little systematic study. Much of the work that has appeared concerns the mutual recognition properties of nitroanilines (Panunto, Zofia, Johnson & Etter, 1987; Etter, Huang, Frankenbach & Asmond, 1991), due to their potential importance in non-linear optical applications, and these authors show that both asymmetric bifurcated [(II),  $X = \text{H}$ ] and mono-coordinate [(III),  $X = \text{H}$ ] motifs are common in this class of compounds.

In light of the previous work on halogen $\cdots\text{O}(\text{nitro})$  interactions and because of the lack of literature data, we have performed a systematic study of hydrogen bonding to nitro-O atoms involving  $\text{N—H}$  or  $\text{O—H}$  donors and using the same techniques as those employed in the halogen $\cdots\text{O}(\text{nitro})$  work. Thus, the present study uses geometrical data on nitro(O) $\cdots\text{H—N,O}$  systems calculated from crystal structures retrieved from the Cambridge Structural Database (CSD: Allen *et al.*, 1991). These geometries are then used to provide suitable starting points for high-level *ab-initio*-based molecular orbital calculations that employ the intermolecular perturbation theory of Hayes & Stone (1984) to study the nature of the interaction energy of a hydrogen-bonded model dimer.

## 2. Methodology

### 2.1. Database analysis

Version 5.11 of the Cambridge Structural Database (April 1996, 154,024 entries) was used in this study. Searches for covalently bonded and hydrogen-bonded substructures, and all geometry calculations, were performed using the program *QUEST3D* (CSD, 1994). Statistical analyses and data visualizations were carried

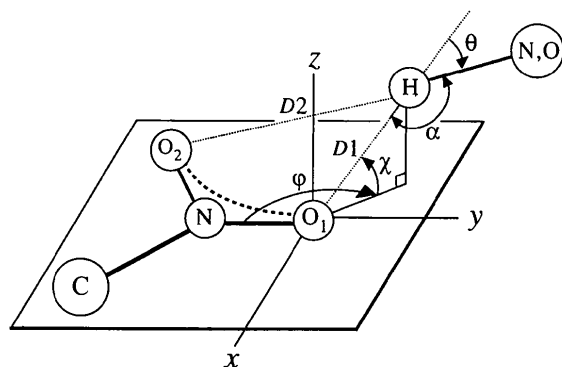


Fig. 1. Geometrical parameters used to describe nitro-O $\cdots\text{H—N,O}$  hydrogen bonds.

Table 1. Summary of search results for nitro-O $\cdots\text{H—N,O}$  hydrogen bonds

All searches are based on those CSD entries that contain both C—NO<sub>2</sub> groups together with either O—H and/or N—H donors

	O—H donors	N—H donors
No. of available NO <sub>2</sub> groups	748	1157
No. of donor H groups available	819	1115
No. of nitro-O $\cdots\text{H}$ interactions $\leq 2.62$ Å (search A)	186	434
No. of unique donor H atoms involved in hydrogen bonds (search B)	164	396
Percentage of donor H atoms forming hydrogen bonds to nitro-O atoms	20.0	35.5

out using *VISTA* (CSD, 1995). All searches were restricted to those CSD entries that satisfied the following secondary search criteria: (a) error-free coordinate set after CSD evaluation procedures, (b) no reported structural disorder, (c) organic compounds according to CSD chemical class definitions and (d)  $R \leq 0.075$ .

Hydrogen-bonded substructures were accepted for analysis if one of the non-covalent N—O $\cdots\text{H}$  distances  $D1 \leq 2.62$  Å, i.e. the upper limit is the sum of the van der Waals radii  $v(\text{O}) = 1.52$  Å (Bondi, 1964),  $v(\text{H}) = 1.10$  Å (Rowland & Taylor, 1996). Only N—H and O—H donors forming intermolecular hydrogen bonds were considered and the donor H atoms were repositioned along the experimentally determined N,O—H bond vectors by the software so that N,O—H bond lengths corresponded to mean values established from neutron studies (Allen *et al.*, 1987). The geometrical parameters illustrated in Fig. 1 were calculated for each hit. The angular parameters  $\chi$  and  $\phi$  describe the geometry of H-atom approach to the C—NO<sub>2</sub> plane, with positive values of  $\phi$  chosen to describe the bifurcated motifs [(I) and (II)], hence negative values of  $\phi$  describe the mono-coordinate motif (III), so as to afford a direct comparison with the study of NO<sub>2</sub> $\cdots$ halogen interactions (Allen, Lommerse, Hoy, Howard & Desiraju, 1997). Due to the possibility of exact or near exact  $C_{2v}$  symmetry of interaction motif (I), both  $D1$  and  $D2$  may satisfy the 2.62 Å search criterion. Thus, two data sets were constructed: (A) containing all examples of  $D1$  or  $D2 \leq 2.62$  Å and (B) containing only those interactions for which  $D1 < D2$ . This latter dataset indicates, of course, how many individual donor H atoms form hydrogen bonds to the available nitro groups. Search results are summarized in Table 1, with mean values of geometrical parameters for datasets A and B being given in Table 2.

### 2.2. Molecular orbital calculations

The intermolecular perturbation theory (IMPT) of Hayes & Stone (1984), as implemented within the *CADPAC6.0* program package (Amos, 1994), was used

Table 2. Mean values of geometrical parameters describing nitro-O...H—N,O hydrogen bonds

Geometrical parameters are illustrated in Fig. 1. For search *A* results,  $\langle D1 \rangle$  includes any nitro-O...H distance that is less than 2.62 Å; search *B* results are for  $D1 \leq 2.62$  Å, where *D1* is the shortest of the two nitro-O...H distances. *N* is the number of observations contributing to each mean value,  $N_N$  and  $N_O$  are the numbers of N—H or O—H donors in any subgroup. Distances are in Å and angles in °, with e.s.d.'s of mean values ( $\sigma$ ) in parentheses. The sample standard deviation (*S*), which provides an indication of the spread of each distribution, is given by  $S = \sigma(N)^{1/2}$  (or  $N_N^{1/2}$  or  $N_O^{1/2}$  if applicable).

Parameter	Search <i>A</i>	Search <i>B</i>	Search <i>B</i> [motifs (I) and (II)]	Search <i>B</i> [motif (III)]
		All data	$90 \leq \varphi \leq 150$	$-150 \leq \varphi \leq -90$
<i>N</i>	620	560	274	183
$N_N$	434	396	194	131
$N_O$	186	164	80	52
$\langle D1 \rangle$ (any donor)	2.30 (1)	2.28 (1)	2.22 (1)	2.34 (1)
$\langle D1 \rangle$ (N—H donors)	2.32 (1)	2.30 (1)	2.26 (1)	2.35 (1)
$\langle D1 \rangle$ (O—H donors)	2.26 (2)	2.23 (2)	2.14 (2)	2.31 (2)
$\langle \alpha \rangle$ (any donor)†	138.9 (8)	139.0 (8)	145.9 (12)	129.1 (11)
$\langle  \chi  \rangle$ (any donor)†	19.4 (7)	20.4 (7)	15.8 (8)	22.2 (12)
$\langle  \varphi  \rangle$ (any donor)†	123.9 (10)	128.2 (10)	117.1 (9)	129.2 (8)

† Mean values of the angular parameters  $\alpha$ ,  $|\chi|$  and  $|\varphi|$  for the individual (N—H or O—H) donor subgroups do not vary significantly from the overall mean values and are not given here.

to quantify the N—O...H hydrogen-bond energies. Application of the IMPT method within *CADPAC6.0* is fully described elsewhere (Lommerse, Stone, Taylor & Allen, 1996; Allen, Lommerse, Hoy, Howard & Desiraju, 1997) and only brief details are given here. For the model molecules used in this study, nitromethane and methanol, 6-31G\*\* basis set functions were used containing polarization functions for both the H and non-H atoms. Model monomers were constructed and geometry optimized. Interacting dimers were then constructed having various orientations of the O—H donor with respect to the nitro group. Intermolecular distances, other than those between the O—H donor group and the nitro-O acceptor of the dimer, were kept as long as possible to minimize non-hydrogen-bond contributions to the total interaction energy. The IMPT method yields separate interaction energy terms which have distinct physical significance, and the sum of these terms yields a total interaction energy,  $E_t$ , which is free of basis set superposition errors (Stone, 1993). At first order, the separate terms are  $E_{es}$ , the (attractive or repulsive) electrostatic energy, and  $E_{er}$ , the exchange-repulsion term. At second order the IMPT gives the polarization or induction energy  $E_{pol}$ , the charge-transfer energy  $E_{ct}$  and the dispersion energy  $E_{disp}$ .

All searches, data analyses and molecular orbital calculations were carried out on SUN or Silicon Graphics workstations on the CCDC Unix network.

### 3. Analysis of crystal structure results

#### 3.1. Frequency of formation and lengths of nitro-O...H bonds

The overall search results show that 29% of the N—H or O—H donors that co-occur with C—NO<sub>2</sub> groups in crystal structures actually form hydrogen bonds to nitro-

O atoms within  $D1 < 2.62$  Å. Donors forming symmetric bifurcated hydrogen bonds [motif (I)] are counted only once. The breakdown of Table 1 shows that the frequency of hydrogen-bond formation by O—H donors (20%) is less than that by N—H donors (36%). All these frequencies are much lower than the 66% of  $>C=O$  groups found to form N—H...O or O—H...O hydrogen bonds by Allen, Bird, Rowland & Raithby (1997). While these statistics do not take account of other acceptors that may be present in individual crystal structures, or the steric availabilities of donors and acceptors, the large frequency difference provides a clear indication that

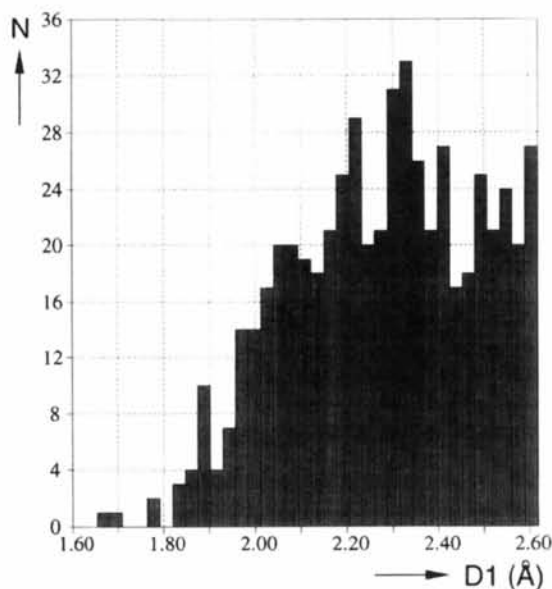


Fig. 2. Histogram of nitro-O...H—N,O hydrogen-bond lengths (*D1*) from search *B* (see text).

hydrogen bonds involving nitro-O atoms are significantly weaker than those involving the  $>C=O$  acceptor.

Further evidence for the relative weakness of nitro- $O \cdots H-N, O$  bonds arises from a comparison of their  $O \cdots H$  distances with those in  $>C=O \cdots H-N, O$  systems. The histogram of  $D1$  for the 560 nitro- $O \cdots H$  contacts of search  $B$  is shown in Fig. 2. There is no clear hydrogen-bonding region (even if higher  $D1$  limits are taken), as there is for  $>C=O \cdots H$  systems. Further, the mean nitro- $O \cdots H-O$  and nitro- $O \cdots H-N$  distances, 2.23 (2) and 2.30 (2) Å, respectively (Table 2), are very significantly longer than the corresponding data for their  $>C=O \cdots H-O$  (5861 observations) and  $>C=O \cdots H-N$  (7014 observations) counterparts, 1.884 (3) and 2.011 (2) Å (Allen, Bird, Rowland & Raithby, 1997), mean values that were also obtained within an  $O \cdots H$  limit of 2.62 Å.

### 3.2. Motif formation, motif geometry and directionality of H approach to O(nitro)

The spherical polar angles  $\chi$  and  $\varphi$  (Fig. 1) describe the orientation of the  $H \cdots O$  vector with respect to the  $C-NO_2$  plane. The sign of  $\chi$  is not discriminatory here and  $|\chi|$  absolute values are used throughout. However, the sign of  $\varphi$  is important:  $\varphi$  is measured in-plane and relative to the unique  $N-O1$  vector established by the search criteria. Thus (Fig. 1), positive  $\varphi$  values place the incoming H atom *trans* to the C atom about  $N-O1$ , corresponding to bifurcated motifs (I) and (II), whereas negative  $\varphi$  values place H in a *cis* relationship to C, as in motif (III). A circular scatterplot of  $\varphi$  versus  $(1 - \sin |\chi|)^{1/2}$  is shown in Fig. 3, where the use of  $(1 - \sin |\chi|)^{1/2}$  (Allen, Lommerse, Hoy, Howard & Desiraju,

1997) generates an equal-area projection (Fisher, Lewis & Embleton, 1987) of the  $|\chi|$  distribution, *i.e.* one in which equal areas on the hemisphere of hydrogen approach map to equal areas on the circle of projection. The view is along the perpendicular to the  $C-NO_2$  plane through O1 and lower  $|\chi|$  values populate the outer edges of the plot, moving in towards values of  $|\chi| = 90^\circ$  at the centre.

Fig. 3 shows a preference for hydrogen-bond formation *via* the bifurcated motifs (I) and (II); 274 (49%) of the independent donor H atoms show  $\varphi$  in the range  $90-150^\circ$ , while 183 (33%) show  $\varphi$  in the range  $-150$  to  $-90^\circ$ , which corresponds to the mono-coordinate motif (III). However, only 60 donor H atoms form interactions in which contacts to both nitro-O atoms are less than 2.62 Å and there are only five examples of near-symmetric bifurcation having  $D2 - D1 < 0.05$  Å. Obviously, these 60 strongly bifurcated examples occur at the lower end of the  $+\varphi$  range, between  $\varphi = 88$  and  $110^\circ$ . Beyond that point, it is clear that H interacts more strongly with one nitro-O atom than the other.

Mean values of geometrical parameters for these two separate  $\varphi$ -ranges are included in Table 2 and a number of significant differences exist between the geometries of the two motifs. (a) The nitro- $O \cdots H$  distances are consistently shorter in motifs (I) and (II). (b) Fig. 3 and the  $\langle |\chi| \rangle$  values show that H approaches O in motifs (I) and (II) at angles which are closer to the  $C-NO_2$  plane than in motif (III). (c) The  $\langle |\varphi| \rangle$  value for motifs (I) and (II) [ $117.1 (9)^\circ$ ] implies that lone-pair directionality involving one of the nitro-O atoms is responsible for the consistent asymmetry of  $D1$  and  $D2$  in this motif. By comparison, the  $\langle |\varphi| \rangle$  value for motif (III) [ $129.2 (8)^\circ$ ] is rather large. (d) The value of  $\langle \alpha \rangle$ , the angle at H in the  $O \cdots H-N, O$  bond, is closer to  $180^\circ$  in motifs (I) and (II) than it is in motif (III). Bearing in mind that it is geometrically impossible to achieve linearity at H in the symmetric or near-symmetric bifurcated motif (I), then the mean value of  $\alpha$  [ $129.1 (11)^\circ$ ] in motif (III) is relatively low, given that steric control of the geometry is less obvious.

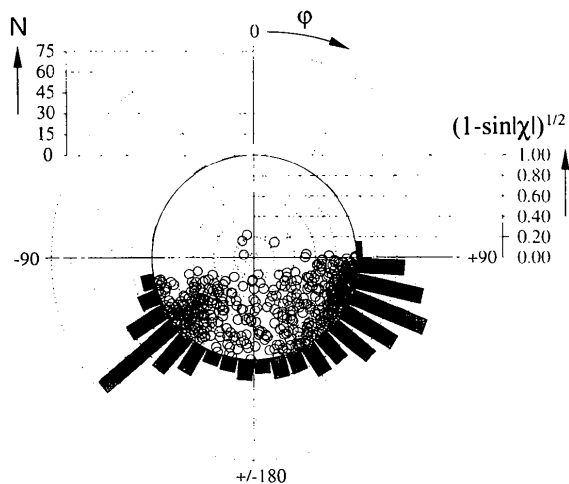


Fig. 3. Circular scattergram of  $(1 - \sin |\chi|)^{1/2}$  versus  $\varphi$  (see text), illustrating the direction of approach of donor H to nitro-O atoms. Lower  $|\chi|$  values populate the circumference of the plot with  $\chi = 90^\circ$  at its centre. The  $N-O1$  vector is at  $\varphi = 0^\circ$  with O1 at the origin. O2 is at positive  $\varphi$  and the nitro-C substituent is at negative  $\varphi$ .

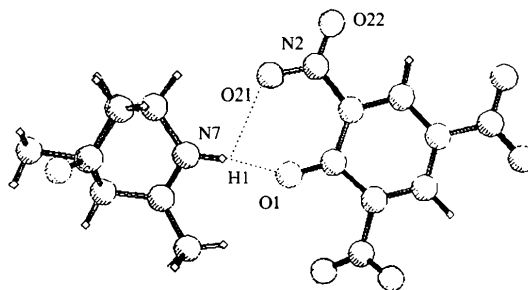


Fig. 4. Steric and (here) electrostatic factors affect the geometry of mono-coordinate motif (III) hydrogen bonding to nitro-O atoms (example from CSD reference code CLJXOI: Robertson, Tooptakong, Lamberton & Geewanda, 1984).

The results (a)–(d) above led us to examine the donor H-atom environment in examples of the mono-coordinate motif (III). Importantly, as with the C—NO<sub>2</sub>···halogen interactions studied previously (Allen, Lommerse, Hoy, Howard & Desiraju, 1997), the majority of nitro groups are attached to coplanar phenyl rings and similar conjugated systems. This means that substituents, even H, *ortho* to the nitro group can act to prevent in-plane approach of donor-H to the nitro-O along the lone-pair direction and can obviously distort the donor-H···O angle away from linearity. Further, a significant number of cases were located in which the *ortho* substituent was itself a strong hydrogen-bond acceptor and one such example (Robertson, Tooptakong, Lamberton & Geewanda, 1984) is depicted in Fig. 4. Here the donor N—H forms a strong and almost linear hydrogen bond to the keto oxygen, leading to severe geometrical distortions in the secondary and hydrogen-bifurcated N—H···O(nitro) interaction, which nevertheless appears in our analysis as an example of the mono-coordinated motif (III).

#### 4. Molecular orbital calculations

##### 4.1. Choice of model monomers and dimers

The simplest model molecules, nitromethane and methanol, were chosen for IMPT calculations. As noted in the earlier work on nitro-O···halogen interactions (Allen, Lommerse, Hoy, Howard & Desiraju, 1997), a high proportion of nitro groups in the CSD are attached to aromatic systems and, hence, nitrobenzene would have been a more natural choice of model. However, this introduces significant computational overheads: each individual, fixed-geometry IMPT calculation takes *ca* 10 h c.p.u. time on a Silicon Graphics Indigo-2 workstation for the nitrobenzene–methanol model, instead of the *ca* 45 min required for the smaller system. In any case, use of the C(alkyl) system still reflects the overall hydrogen-bonding capability of the nitro-O atoms: 109 of the 560 unique interactions of search *B* (Tables 1 and 2) have C(alkyl) substituents and the approximate 3:2 preference for motif (I) exhibited by the full dataset is preserved here.

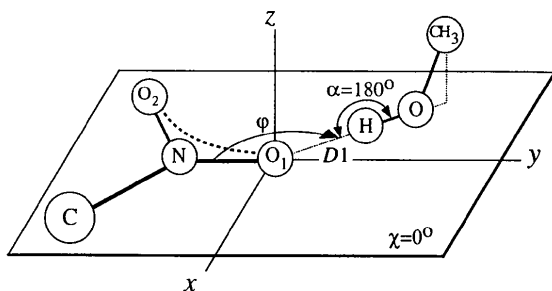


Fig. 5. The nitromethane–methanol model dimer used in the IMPT calculations.

The model monomer molecules were geometry optimized using 6-31G\*\* basis sets and an initial dimer was then constructed using the geometry depicted in Fig. 5. Here the O—C vector of methanol was placed in the plane perpendicular to the C—NO<sub>2</sub> system. Such an orientation minimizes other non-bonded interactions in the dimer, apart from the nitro-O···H—O interaction of interest.

##### 4.2. IMPT calculations

IMPT calculations were principally carried out to study variations in the individual energy terms and, of course, the total energy profile,  $E_t$ , as a function of the parameters  $D1$  and  $\varphi$  (see Fig. 1). The nitro-O···H—O(methanol) angle ( $\alpha$ ) and the hydrogen approach angle ( $\chi$ ) were kept fixed at 180° (linear hydrogen bond) and 0° (in-plane hydrogen approach) throughout these calculations. IMPT energies were calculated at 15  $\varphi$  values ( $\pm 105$ , 120, 125, 130, 135, 150, 165° and the unique 180° position) for each of the O···H distances  $D1 = 1.9$ , 2.0, 2.1, 2.2 and 2.3 Å. Plots of the IMPT energy variations with  $\varphi$  at each of these five  $D1$  values are shown in Fig. 6(a)–(e). All these plots show that the interaction is primarily electrostatic in origin and each plot shows two shallow minima in the (attractive) total energy profile,  $E_t$ , at *ca*  $\pm 120$ –130° in  $\varphi$ . These values are close to the expected positions of the O lone pairs and agree well with the crystallographic observations if the steric factors affecting the experimental molecules are taken into account. The  $E_t$  profiles of Fig. 6 differ markedly from those for nitro-O···halogen interactions (Allen, Lommerse, Hoy, Howard & Desiraju, 1997), which do not show O lone-pair directionality.

A study of the energy differences between the two local minima shows some interesting features that are illustrated (Fig. 7) by a superposition of the  $\varphi$ – $E_t$  profiles for the five different  $D1$  values. At  $D1 = 1.9$  Å the mono-coordinate motif (III) (negative  $\varphi$  values,  $E_t = -15.0$  kJ mol<sup>-1</sup>) is preferred to the bifurcated motifs (I) and (II) (positive  $\varphi$  values,  $E_t = -14.2$  kJ mol<sup>-1</sup>) by 0.8 kJ mol<sup>-1</sup>. As  $D1$  increases the local minima first equalize in energy and then, at 2.2 and 2.3 Å, the bifurcated motifs (I) and (II) become energetically favoured, by 0.7 and 1.0 kJ mol<sup>-1</sup>, respectively. It is these longer distances that dominate the histogram of nitro-O···H—O,N distances shown in Fig. 2. The energy differences calculated for these longer  $D1$  values clearly correspond to the preference for bifurcated motifs that is exhibited in the experimental data.

Individual energy minima at the different  $D1$  values are remarkably consistent and range from  $-14.1$  ( $\varphi = 125^\circ$  at  $D1 = 2.3$  Å) to  $-15.4$  kJ mol<sup>-1</sup> ( $\varphi = -125^\circ$  at  $D1 = 2.0$  Å). Thus, the nitro-O···H—O hydrogen bond is about half as strong as a carboxylate C=O···H—O bond (Jeffrey & Saenger, 1991). Further, lone-pair directionality is quite clearly seen in the nitro-O case, in both the experimental and computational results.

In modelling the bifurcated motifs (I) and (II), all of the  $D1-\varphi$  calculations depicted in Figs. 6 and 7 obviously place the donor H atom closer to one of the nitro-O atoms than the other, in agreement with the crystallographic results. In a further IMPT calculation we examined the energetics of the perfectly symmetric bifurcated motif (I) by moving the methanol molecule towards the nitro

group along the extension of the nitromethane C—N bond vector, as shown in Fig. 8. Values of  $d$ , the common nitro-O $\cdots$ H distance, were varied from 2.1 to 2.9 Å in 0.1 Å increments to yield the energy profiles also shown in Fig. 8. The total IMPT energy shows a broad minimum at  $d$  values in the range 2.4–2.6 Å. The energy minimum of  $-11.9$  kJ mol $^{-1}$  at  $d = 2.5$  Å is some 3 kJ mol $^{-1}$

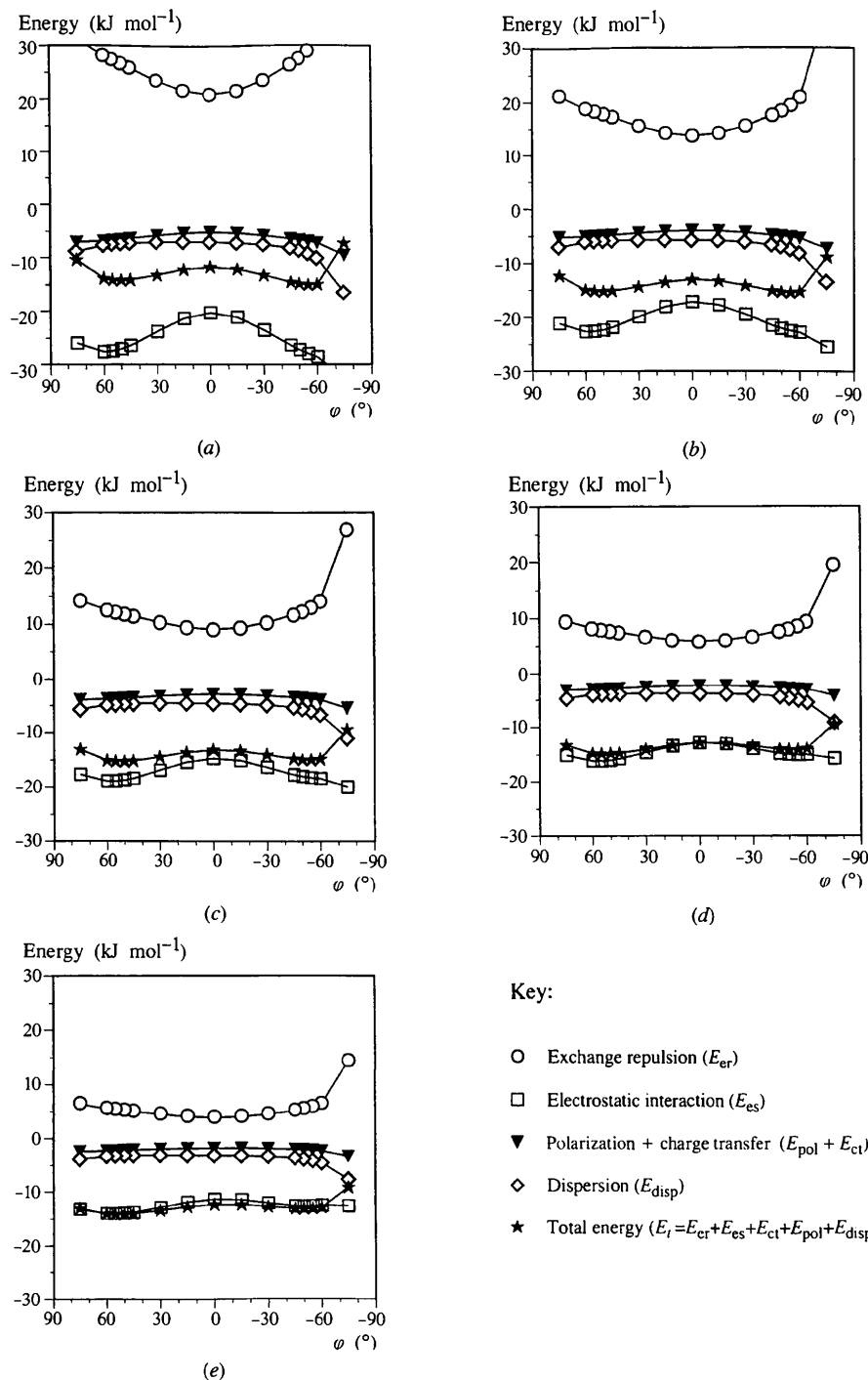


Fig. 6. Variation in IMPT interaction energies with changes in  $\varphi$  at five different values of  $d$ , the O $\cdots$ H hydrogen-bond length: (a)  $d = 1.9$ , (b)  $d = 2.0$ , (c)  $d = 2.1$ , (d)  $d = 2.2$  and (e)  $d = 2.3$  Å.

higher than that obtained for the asymmetric bifurcated motif, and accounts for the paucity of crystallographic examples that adopt a symmetric or near-symmetric bifurcated arrangement. As with the smaller halogens, Cl and Br, it is clearly more energetically favourable for the donor H atom to form one shorter and stronger interaction to an individual nitro-O atom than it is to form a pair of longer and weaker interactions to both nitro-O atoms.

## 5. Conclusions

Crystallographic results and high-level molecular orbital calculations for  $\text{N}_2\text{O}-\text{H}\cdots\text{O}(\text{nitro})$  systems are in excellent agreement at a detailed level. The essential conclusions of this combined study are: (a) the donor H atom prefers to approach the nitro-O atom in the  $\text{C}-\text{NO}_2$  plane. (b) An approximately 3:2 preference for the bifurcated motifs (I) and (II) over the mono-coordinate motif (III) exhibited in the crystallographic data corresponds to an energetic preference of  $0.7\text{--}1.0\text{ kJ mol}^{-1}$  given by the IMPT calculations at  $D1 = 2.2\text{--}2.3\text{ \AA}$ . (c) There is clear evidence for O lone-pair directionality in both the crystallographic and computational results, however, the crystallographic geometries of mono-coordinate motifs (III) are distorted by unfavourable steric interactions and, in some cases, additional hydrogen bonding to neighbouring atoms in the experimental molecules. (d) There are relatively few crystallographic examples of true hydrogen bonding to both nitro-O atoms in bifurcated motifs (I): the donor H atom prefers to form a single short interaction with an individual nitro-O atom. The IMPT calculations show that asymmetric bifurcated motifs (II) are favoured by *ca*  $3\text{ kJ mol}^{-1}$  over their perfectly symmetrical counterparts (I). (e) The crystallographic data indicates that  $\text{nitro-O}\cdots\text{H}-\text{N}_2\text{O}$  bonds are significantly weaker than comparable bonds involving stronger acceptors, *e.g.*  $>\text{C}=\text{O}$  in ketones, carboxylates and amides, and the IMPT calculations provide an interaction energy of *ca*  $-15\text{ kJ mol}^{-1}$  for the nitro acceptor.

We thank Drs Anthony Stone and Roger Amos (University of Cambridge) for access to *CADPAC6.0* and for assistance and advice on the IMPT method. We also thank the European Communities for financial support to JPML under the Training and Mobility of Researchers Programme, Contract No. ERB-CHR-XT-94-0469 (Molecular Recognition Network).

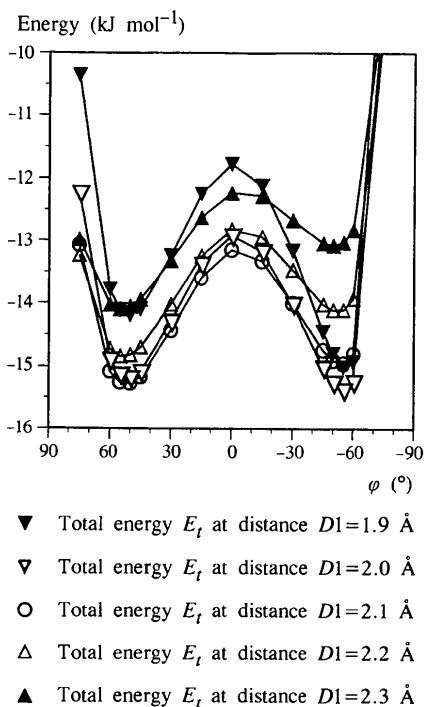


Fig. 7. Superposition of the  $E_t$ - $\phi$  energy profiles for the five different  $d$  values used in Fig. 6.

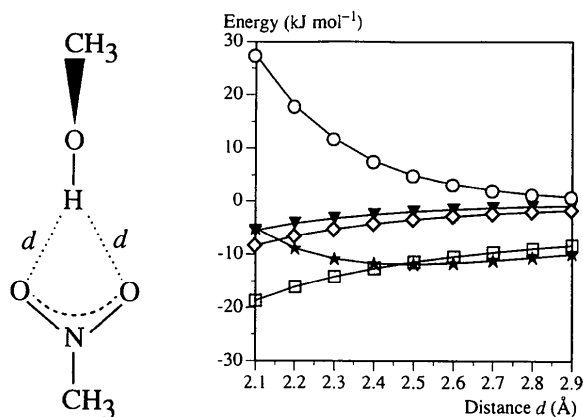


Fig. 8. Variation in IMPT interaction energies with  $d$  for the perfectly symmetrical bifurcated hydrogen-bond motif (I) (see Fig. 6 for an explanation of the graphical symbols).

## References

- Allen, F. H., Bird, C. M., Rowland, R. S. & Raithby, P. R. (1997). *Acta Cryst.* **B53**, 680–695.  
 Allen, F. H., Davies, J. E., Galloy, J. J., Johnson, O., Kennard, O., Macrae, C. F., Mitchell, E. M., Mitchell, G. F., Smith, J. M. & Watson, D. G. (1991). *J. Chem. Inf. Comput. Sci.* **31**, 187–204.  
 Allen, F. H., Goud, B. S., Hoy, V. J., Howard, J. A. K. & Desiraju, G. R. (1994). *Chem. Commun.* pp. 2729–2730.  
 Allen, F. H., Kennard, O., Taylor, R., Watson, D. G., Orpen, A. G. & Brammer, L. (1987). *J. Chem. Soc. Perkin Trans. 2*, pp. S1–S19.  
 Allen, F. H., Lommerse, J. P. M., Hoy, V. J., Howard, J. A. K. & Desiraju, G. R. (1997). *Acta Cryst.* **B53**, 1006–1016.  
 Amos, R. D. (1994). *CADPAC6.0. The Cambridge Analytical Derivatives Package. Issue 6.0. A Suite of Quantum Chemistry programs.* University of Cambridge, England.

- Bondi, A. (1964). *J. Phys. Chem.* **68**, 441–451.
- Cambridge Structural Database (1994). *User's Manual. Getting Started with the CSD System*. Cambridge Crystallographic Data Centre, 12 Union Road, Cambridge, England.
- Cambridge Structural Database (1995). *VISTA2.0 User's Manual*. Cambridge Crystallographic Data Centre, 12 Union Road, Cambridge, England.
- Desiraju, G. R. (1995). *Angew. Chem. Int. Ed. Engl.* **34**, 2311–2327.
- Etter, M. C., Huang, K. S., Frankenbach, G. M. & Asmond, D. A. (1991). *Am. Chem. Soc. Symp. Ser.* **455**, 446–456.
- Fisher, N. I., Lewis, T. & Embleton, B. J. J. (1987). *Statistical Analysis of Spherical Data*. Cambridge University Press.
- Hayes, I. C. & Stone, A. J. (1984). *J. Mol. Phys.* **53**, 83–105.
- Jeffrey, G. A. & Saenger, W. (1991). *Hydrogen Bonding in Biological Systems*. Berlin: Springer-Verlag.
- Lommerse, J. P. M., Stone, A. J., Taylor, R. & Allen, F. H. (1996). *J. Am. Chem. Soc.* **118**, 3108–3116.
- Panunto, T. W., Zofia, U., Johnson, R. & Etter, M. C. (1987). *J. Am. Chem. Soc.* **109**, 7786–7797.
- Robertson, G. B., Tooptakong, U., Lambertson, J. A. & Geewanda, Y. (1984). *Tetrahedron Lett.* **25**, 2695–2698.
- Rowland, R. S. & Taylor, R. (1996). *J. Phys. Chem.* **100**, 7384–7391.
- Stone, A. J. (1993). *Chem. Phys. Lett.* **211**, 401–409.
- Thalladi, V. R., Goud, B. S., Hoy, V. J., Allen, F. H., Howard, J. A. K. & Desiraju, G. R. (1996). *Chem. Commun.* pp. 401–402.